Published in final edited form as:
Fitoterapia. 2014 March ; 93: 194–200. doi:10.1016/j.fitote.2013.12.013.

Bioactive sesquiterpene lactones and other compounds isolated from *Vernonia cinerea*

Ui Joung Youn[a], **Gabriella Miklossy**[b], **Xingyun Chai**[a], **Supakit Wongwiwatthananukit**[c], **Onoomar Toyama**[d], **Thanapat Songsak**[e], **James Turkson**[b], and **Leng Chee Chang**[a,*]

[a]Department of Pharmaceutical Sciences, Daniel K. Inouye College of Pharmacy, University of Hawai'i at Hilo, Hilo, HI, 96720, United States [b]Natural Products and Experimental Therapeutics Programs, University of Hawai'i Cancer Center, Honolulu, HI, 96813, United States [c]Department of Pharmacy Practice, Daniel K. Inouye College of Pharmacy, University of Hawai'i at Hilo, Hilo, HI, 96720, United States [d]Department of Pharmaceutical Chemistry, Faculty of Pharmacy, Silpakorn University, Nakhon Pathom 73000, Thailand [e]Department of Pharmacognosy, Faculty of Pharmacy, Rangsit University, Pathumtani 12000, Thailand

Abstract

Four new sesquiterpene lactones, 8*α*-(2′*Z*-tigloyloxy)-hirsutinolide (**1**), 8*α*-(2′*Z*-tigloyloxy)-hirsutinolide-13-*O*-acetate (**2**), 8*α*-(4-hydroxytigloyloxy)-hirsutinolide (**3**), and 8*α*-hydroxy-13-*O*-tigloyl-hirsutinolide (**4**), along with seven known derivatives (**5**–**11**), three norisoprenoids (**12**–**14**), a flavonoid (**15**), and a linoleic acid derivative (**16**), were isolated from the chloroform partition of a methanol extract from the combined leaves and stems of *Vernonia cinerea*. Their structures were established by 1D and 2D NMR, UV, and MS analyses. Compounds **1**–**16** were evaluated for their inhibitory effects against the viability of U251MG glioblastoma and MDA-MB-231 breast cancer cells that harbour aberrantly-active STAT3, compared to normal NIH3T3 mouse fibroblasts that show no evidence of activated STAT3. Among the isolates, compounds **2** and **7** inhibited the aberrant STAT3 activity in glioblastoma or breast cancer cells. Further, compounds **7** and **8** inhibited viability of all three cell lines, compounds **2**, **4**, and **9** predominantly inhibited the viability of the U251MG glioblastoma cell line.

Keywords

Vernonia cinerea; Asteraceae; Sesquiterpene lactone; STAT3

1. Introduction

The search for genes that control tumor growth and progression has resulted in the discovery of oncogenes, which are subject to mutational activation in cancer cells, as well as tumor

*Corresponding author: Tel.: +1 808 981 8018; fax: +1 808 933 2974. lengchee@hawaii.edu (L.C. Chang).

Conflict of interest
The authors declare no conflict of interest.

suppressors [1]. However, not all oncogenes are targets for mutational activation. Notable examples are the NF-κB and STAT3 transcriptional factors which were found to play pivotal roles in various aspects of the tumorigenic process in a number of malignancies [2,3]. Most often, NF-κB and STAT3 are constitutively activated in neoplastic cells due to upregulation of upstream signaling pathways in response to autocrine and paracrine factors that are produced within the tumor microenvironment [4]. Although NF-κB and STAT3 do not match the classical oncogene definition, they are powerful activators of the malignant state and control expression of target genes important for cell proliferation, survival, angiogenesis and tissue repair [5–8]. However, the functions of NF-κB and STAT3 extend far beyond the cancer cell and both transcriptional factors are important regulators of immune and inflammatory functions [9,10]. While being activated by cytokines and growth factors, both NF-κB and STAT3 control the expression of other cytokines and inflammatory/immune mediators, thus serving as a regulatory hub that coordinates immune and inflammatory responses. Therefore, NF-κB and STAT3 also affect cancer cell physiology through their effects on immune and inflammatory cells in the tumor microenvironment [11–13].

As part of an effort to discover naturally occurring anticancer agents and STAT3 inhibitors from tropical plants, a methanol extract from the combined leaves and stems of *V. cinerea* was evaluated and found to exhibit an inhibitory effect against the STAT3 activity in the U251MG glioblastoma and MDA-MB-231 breast cancer cells, and to promote the loss of viability of the two tumor cells *in vitro*, and not of normal NIH-3 T3 mouse fibroblasts.

V. cinerea Less (Asteraceae) is an annual herb that grows in South-East Asia, India and China [14,15]. It is used for malaria, pain, inflammation, infections, diuresis, cancer, abortion, and various gastro-intestinal disorders [16–21]. In particular, the root of this plant has bitter and is used as an anthelmintic and diuretic [22]. Fresh juice of leaves is given to treat dysentery and is locally applied for the extraction of guinea worms [22]. The seeds are also used as an anthelmintic and alexipharmic, and they are known to be quite effective against round worms and thread worms [22]. Aqueous ethanolic extracts (50%) of this plant were found to possess activity against ranikhet virus disease [23]. The phytochemicals previously reported from *V. cinerea* include sesquiterpene lactones, steroidal glycosides, triterpenoids, and flavonoids [18,24–26]. In our previous studies on bioactive constituents from the flowers of *V. cinerea*, we reported isolating the sesquiterpene lactones, and determined their anti-inflammatory activities [27].

This paper reports the isolation and structure elucidation of the new sesquiterpene lactones, **1**–**4**, together with twelve known compounds (**5**–**16**), as well as their ability to inhibit STAT3 activity and promote antitumor cell effects *in vitro* against human glioma and breast cancer cells.

2. Experimental

2.1. General experimental procedures

Optical rotations were measured on a Rudolph Research Autopol IV multiwavelength polarimeter. UV spectra were run on a Shimadzu PharmaSpec-1700 UV–visible

spectrophotometer. CD spectra were recorded on a JASCO J-815 spectropolarimeter. IR spectra were measured on a Bruker Tensor-27 FT-IR spectrometer. NMR spectroscopic data were recorded at room temperature on a Bruker Avance DRX-400 spectrometer, and the data were processed using TopSpin 3.1 software. High-resolution electrospray ionization mass spectra (HRESIMS) were obtained with an Agilent 6530 LC-qTOF High Mass Accuracy mass spectrometer operated in the positive- and negative-ion modes. Analytical TLC was performed on 0.25 mm thick silica gel F_{254} glass-backed plates (Sorbent Technologies). Column chromatography was carried out with silica gel (230–400 mesh; Sorbent Technologies) and RP-18 (YMC · GEL ODS-A, 12 nm, S-150 μm) was used for column chromatography. Semipreparative (10 × 150 mm) columns were used for semipreparative HPLC, and were conducted on a Beckman Coulter Gold-168 system equipped with a photodiode array detector using an Alltech reversed-phase Econosil C-18 column (10 μm, 10 × 250 mm) with a flow rate of 1.5 mL/min.

2.2. Plant material

The leaves and stems of *V. cinerea* were provided by Lampang Herb Conservation Club, Lampang Province, Thailand, in May 2011. The plant materials were identified by Dr. Thanapat Songsak, (Faculty of Pharmacy, Rangsit University). A voucher specimen (No. VCW02) was deposited at the Natural product chemistry Laboratory, College of Pharmacy, University of Hawaii at Hilo.

2.3. Extraction and isolation

The air-dried and finely ground combination of the leaves and stems of *V. cinerea* (10 kg) was extracted by maceration in MeOH (3 × 40 L) at room temperature. The solvent was concentrated in vacuo to yield 774 g of a crude extract, which was then suspended in distilled water (4 L) and then extracted successively with $CHCl_3$ (3 × 4 L), EtOAc (3 × 4 L), and *n*-butanol (3 × 4 L). The $CHCl_3$-soluble extract (300 g), was separated by column chromatography over Si gel (CC; φ20 cm; 230–400 mesh, 5 kg) using a gradient solvent system of n-hexane–EtOAc (100:1 to 0:100), to afford 16 fractions (C1–C16). Fraction C2 (78 g) was subjected to Si gel (CC; φ10 cm; 230–400 mesh, 1 kg), with n-hexane–EtOAc (100:0 to 1:1) as the solvent system, yielding fifteen subfractions (C2.1 to C2.15). Combined subfractions C2.12 and C2.13 (1.5 g) were chromatographed over an open C_{18} column, eluted with H_2O–MeOH solvents (90:10 to 100% MeOH), to afford five subfractions (C2.12.1 to C2.12.5). Subfraction C2.12.2 (0.8 g) was purified by HPLC on a semipreparative RP-18 column, using MeOH–H_2O mixtures (60:40 to 0:100) as the solvent system, to yield **6** (25 mg, t_R 119 min), **7** (50 mg, t_R 121 min), **9** (20 mg, t_R 124 min), and **11** (22 mg, t_R 127 min). Subfraction C2.12.3 (0.3 g) was purified by HPLC on a semipreparative RP-18 column, using MeOH–H_2O mixtures (60:40 to 0:100) as the solvent system, to yield **5** (24 mg, t_R 86 min), **1** (2 mg, t_R 96 min), and **8** (4.5 mg, t_R 99 min). Subfraction C2.14 (2.0 g) was chromatographed over an open C_{18} (400 g) column and eluted with H_2O–MeOH mixtures (90:10 to 100% MeOH), to afford three subfractions (C2.14.1 to C2.14.3). Subfractions C2.14.1 and C2.14.2 (0.8 g) were purified by HPLC on a semipreparative RP-18 column, using MeOH–H_2O mixtures (60:40 to 0:100) as the solvent system, to yield, in turn, **10** (102 mg, t_R 78 min), **2** (1.5 mg, t_R 115 min), **12** (6 mg, t_R 122 min), **13** (3 mg, t_R 123 min), and **9** (4 mg, t_R 125 min). Subfraction C2.15 (4.0 g) was

chromatographed on an open C_{18} (400 g) column and eluted with H_2O–MeOH (90:10 to 100% MeOH), to afford four subfractions (C2.15.1 to C2.15.4). Subfraction C2.15.1 (0.4 g) was subjected to separation on a semipreparative RP-18 column by HPLC, using MeOH–H_2O mixtures (60:40 to 100:0) as solvent system, to yield **5** (10 mg, t_R 85 min), **1** (3 mg, t_R 95 min), **14** (5 mg, t_R 97 min), and **6** (30 mg, t_R 105 min). Subfraction C2.15.2 (0.5 g) was subjected to semipreparative HPLC (MeOH–H_2O = 50:50 to 100:0), to yield **4** (2.5 mg, t_R 88 min), **15** (8 mg, t_R 90 min), **8** (3 mg, t_R 100 min), **11** (10 mg, t_R 93 min), and **7** (30 mg, t_R 105 min). Fraction C14 (10 g) was chromatographed on a Sephadex LH-20 gel (300 g) column and eluted with H_2O–MeOH (100:0 to 50:50) solvent system, to afford nine subfractions (C14.1 to C14.9). Compound **3** (2 mg, t_R 90 min) was purified from subfraction C14.3 (0.1 g) by semipreparative RP-18 column and HPLC methods, using (MeOH–H_2O = 50:50 to 80:20) as solvent system. Compound **16** (10 mg) was crystallized in MeOH–$CHCl_3$ (1:2) from the subfraction C15.

2.3.1. 8α-(2′Z-Tigloyloxy)hirsutinolide (1)—White amorphous powder; $[\alpha]_D^{20} = +28.5^\circ$ (*c* 0.2, MeOH); UV (MeOH) λ_{max} (log ε) 290 (4.0) nm; CD (*c* 0.1, MeOH) 289 (+35.3); IR ν_{max} (KBr) 3320, 1760 $cm^{-1;}$ ^1H (400 MHz) and ^{13}C NMR (100 MHz) data, see Table 1; HRESIMS *m/z* 401.1724 $[M + Na]^+$ (calcd for $C_{20}H_{26}O_7Na$, 401.1726).

2.3.2. 8α-(2′Z-Tigloyloxy)hirsutinolide-13-O-acetate (2)—White amorphous powder; $[\alpha]_D^{20} = +20.3^\circ$ (*c* 0.2, MeOH); UV (MeOH) λ_{max} (log ε) 290 (4.2) nm; CD (*c* 0.1, MeOH) 289 (+36.6); IR ν_{max} (KBr) 3335, 1760 $cm^{-1;}$ ^1H (400 MHz) and ^{13}C NMR (100 MHz) data, see Table 1; HRESIMS *m/z* 443.1817 $[M + Na]^+$ (calcd for $C_{22}H_{28}O_8Na$, 443.1829).

2.3.3. 8α-(4-Hydroxytigloyloxy)-hirsutinolide (3)—White amorphous powder; $[\alpha]_D^{20} = +25.5^\circ$ (*c* 0.2, MeOH); UV (MeOH) λ_{max} (log ε) 288 (4.1) nm; CD (*c* = 0.1, MeOH) 290 (+35.6); IR ν_{max} (KBr) 3330, 1760 $cm^{-1;}$ ^1H (400 MHz) and ^{13}C NMR (100 MHz) data, see Table 2; HRESIMS *m/z* 417.1660 $[M + Na]^+$ (calcd for $C_{20}H_{26}O_8Na$, 417.1672).

2.3.4. 8α-Hydroxy-13-O-tigloyl-hirsutinolide (4)—White amorphous powder; $[\alpha]_D^{20} = +27.7^\circ$ (*c* 0.2, MeOH); UV (MeOH) λ_{max} (log ε) 290 (4.0) nm; CD (*c* = 0.1, MeOH) 294 (+40.3); IR ν_{max} (KBr) 3335, 1760 $cm^{-1;}$ ^1H (400 MHz) and ^{13}C NMR (100 MHz) data, see Table 2; HRESIMS *m/z* 401.1722 $[M + Na]^+$ (calcd for $C_{20}H_{26}O_7Na$, 401.1723).

2.4. Cell viability assay

Cell viability was determined using CyQuant assay according to the manufacturer's (Invitrogen, CA, USA) instructions, as reported previously [28,29]. Cells (U251MG, MDA-MB-231 or NIH3T3) were cultured in 96-well plates at 2000 cells per well for 24 h and subsequently treated with compounds (5 μM) for 72 h and analyzed. Relative viability of the treated cells was normalized to the DMSO-treated control cells.

2.5. Western blotting analysis for pYSTAT3 and STAT3

Whole-cell lysates were prepared in boiling SDS sample loading buffer to extract total proteins, as reported previously [30–32]. Lysates of equal total protein prepared from DMSO- or compound-treated cells were electrophoresed on an SDS-7.5% polyacrylamide gel and transferred to a nitrocellulose membrane. Nitrocellulose membranes were probed with primary antibodies, and the detection of horse-radish peroxidase-conjugated secondary antibodies by enhanced chemiluminescence (Amersham) was performed. Antibodies used were monoclonal anti-pYSTAT3 and anti-STAT3 antibodies (Cell Signaling Technology, Danvers, MA).

3. Results and discussion

The chloroform partition of the combined leaves and stems of *V. cinerea* was repeatedly subjected to column chromatography on silica gel, RP-18 gel, Sephadex LH-20 gel, and preparative HPLC to afford four new sesquiterpene lactones, **1**–**4**, along with twelve known compounds (**5**–**16**) (Fig. 1).

Compound **1** was obtained as a white amorphous powder and gave a molecular ion at *m/z* 401.1724 $[M + Na]^+$ (calcd for $C_{20}H_{26}O_7Na$, 401.1726) in the positive-ion HRESIMS, corresponding to a molecular formula of $C_{20}H_{26}O_7$. The IR absorption band at 1760 cm^{-1} and a strong absorption around 290 nm in the UV spectrum indicated the presence of a conjugated lactone group. The ^{13}C NMR spectrum showed characteristic signals that further supported the γ lactone group [δ_C 169.4 (C-12), 147.5 (C-7), 146.4 (C-6), and 131.6 (C-11)] (Table 1) [24]. The NMR and HSQC spectra revealed two methyls at [δ_H 0.97 (d, J = 6.8 Hz)/δ_C 16.8 (CH_3-14) and δ_H 1.48 (s)/δ_C 27.9 (CH_3-15)], three methylenes at [δ_H 2.16 m/δ_C 38.5 (C-2), δ_H 2.16 m/δ_C 38.6 (C-3), and δ_H 2.36 (dd, J = 15.62, 11.6 Hz, H-9α), 1.87 (m, H-9β)/δ_C 37.9 (C-9)], a methine at δ_H 1.90 (m)/δ_C 41.3 (C-10), an oxymethine downfield shifted at δ_H 6.34 (d, J = 8.0 Hz)/δ_C 68.2 (C-8), and an olefinic signal at δ_H 5.87 (s)/δ_C 125.6 (C-5), all of which suggested the presence of a hirsutinolide-type sesquiterpene [24]. The ^1H NMR spectrum revealed additional oxygenated methylene protons at [δ_H 4.65 (d, J = 13.2 Hz, H-13a) and 4.56 (d, J = 13.2 Hz, H-13b)], which showed two- and three-bond correlation peaks with C-7, C-12, and C-11 in the HMBC spectrum (Fig. 2), and suggested that this oxymethylene group was attached to the γ lactone moiety. In addition, the ^1H and ^{13}C NMR spectra showed an olefinic signal at δ_H 6.17 (q, J = 7.6 Hz)/δ_C 139.9 (C-3′), two methyl groups downfield shifted at [δ_H 2.02 (d, J = 7.6 Hz)/δ_C 15.9 (C-4′) and δ_H 1.93 (s)/δ_C 20.6 (C-5′)], an olefinic quaternary carbon at δ_C 128.2 (C-2′), and an ester carbonyl carbon at δ_C 170.4 (C-1′), that were indicative of a tigloyl moiety based on the HSQC and HMBC analyses. The ^1H and ^{13}C NMR spectra of **1** were almost identical, to those of 8α-tigloyloxy-hirsutinolide [33], with the following exceptions: the signal for an olefinic proton (H-3′) at δ_H 7.03 in 8α-tigloyloxy-hirsutinolide was shifted upfield to δ_H 6.17 in **1**. In contrast, two methyl group protons at δ_H 1.78 (CH_3-4′) and δ_H 1.80 (CH_3-5′) in 8α-tigloyloxy-hirsutinolide were shifted downfield to 2.02 ppm and 1.93 ppm, respectively, in the tigloyl group of **1** (Table 1), implying that the olefinic (C-2′–C-3′) bond was in the *Z* configuration. These observations were further supported by the NOESY correlation between H-3′ and CH_3-5′ (Fig. 3). Additional NOESY correlations between H-8 and H-9β/

H-13 along with the physicochemical data supported the same configurations in the hirsutinolide type of sesquiterpene lactone, and were comparable with literature data [24,27]. In particular, X-ray crystallographic analysis defined the relative configuration of 8α-tigloyloxy-hirsutinolide obtained in our previous work [27]. Therefore, compound **1** is proposed as a new hirsutinolide geometric isomer, 8α-(2′*Z*-tigloyloxy)hirsutinolide.

Compound **2** was obtained as a white amorphous powder. It had a molecular ion at 443.1817 $[M + Na]^+$ (calcd for $C_{22}H_{28}O_8Na$, 443.1829) in the HRESIMS. The ^1H and ^{13}C NMR spectra of **2** were similar to those of **1**, except for an additional methyl group at δ_H 2.10 (3H, s)/δ_C 20.9 and a carbonyl carbon at δ_C 170.7, consistent with an acetyl moiety. The HMBC spectrum showed a correlation peak between the oxymethylene proton (H-13) and the ester carbonyl carbon (δ_C 170.7), suggesting that the acetyl group was attached to an oxygen atom at C-13. The chemical shifts and the NOESY correlation between H-3′ and CH_3-5′ in the tigloyl group supported the *cis* (*Z*) olefinic double bond between C-2′ and C-3′. The stereochemistry of asymmetric carbons of **2** was the same as in **1**, by comparison of the physicochemical data and NOESY correlations of the two compounds. Thus, compound **2** was elucidated as a new geometric isomer, 8α-(2′ *Z*-tigloyloxy)hirsutinolide-13-*O*-acetate.

Compound **3** was obtained as a white amorphous powder and its molecular formula was established as $C_{20}H_{26}O_8$ by HRESIMS (observed, 417.1660; calcd for $[M + Na]^+$ 417.1672). The UV, IR, and NMR spectra of **3** indicated a hirsutinolide skeleton comparable to those of **1** and **2**. However, the ^1H NMR spectrum revealed additional oxygenated methylene protons at δ_H 4.28 (2H, d, J = 6.4 Hz, H-4′), which showed two- and three-bond HMBC correlations with the two olefinic carbons (C-2′ and C-3′), indicating the attachment of an oxymethylene group instead of a methyl group at C-3′ of the tigloyl moiety. The specific splitting pattern and the coupling constant of the olefinic proton (H-3′) at δ_H 7.08 (t, $^3J_{H\text{-}3', H\text{-}4'}$ = 6.4 Hz) appeared to result from coupling with the oxymethylene proton (H-4′), and further supported the presence of the 4-hydroxytigloyl moiety (Table 2). In addition, the HMBC correlation observed between H-8 and the ester carbonyl carbon (C-1′) demonstrated that the 4-hydroxytigloyl group was attached to C-8 of the sesquiterpene lactone molecule. The relative stereochemistry of **3** was determined in a manner similar to those of **1** and **2**. Accordingly, compound **3** is proposed as a new compound, 8α-(4-hydroxytigloyloxy)-hirsutinolide.

Compound **4** was obtained as a white amorphous powder with a molecular ion at *m/z* 401.1722 $[M + Na^+]$ (calcd for $C_{20}H_{26}O_7Na$, 401.1723) in the HRESIMS, corresponding to an elemental formula of $C_{20}H_{26}O_7$. The 1D and 2D NMR spectra of **4** showed a (2′*E*)-tigloyl moiety, three methylenes, two methyls, an olefinic, an oxymethine, and a γ lactone group, indicating a hirsutinolide-type sesquiterpene lactone, initially assumed from the spectra data to be similar to 8α-tigloyloxyhirsutinolide (**6**) [33]. However, the ^1H NMR spectrum of **4** showed an additional hydroxyl proton doublet at δ_H 6.15 (1H, d, J = 11.6 Hz), which correlated with C-7/C-8/C-9 in the HMBC spectrum (Fig. 2), indicating that the hydroxyl group was connected to C-8. In addition, magnetically equivalent oxygenated methylene protons at δ_H 4.97 (2H, s, H-13) were observed in the ^1H NMR spectra, which also showed a three-bond correlation with a lactone carbonyl carbon (C-12) and an ester carbonyl carbon (C-1′) of the tigloyl moiety in the HMBC spectrum. These observations

unambiguously indicated that the tigloyl group was attached at C-13 through an oxygen atom (Fig. 2). The NOESY correlation peaks between α-oriented OH-8 proton and H-9α, and between H-13 and H-8 (Fig. 3), along with the physicochemical analyses of **4** supported the same relative configurations compared to those of **1**–**3**. Therefore, the structure of **4** was established as a new compound, 8α-hydroxy-13-*O*-tigloyl-hirsutinolide.

The other twelve isolates were identified as the known compounds, 8α-(2-methylacryloyloxy)-hirsutinolide (**5**) [33], 8α-tigloyloxyhirsutinolide (**6**) [33], 8α-tigloyloxyhirsutinolide-13-*O*-acetate (**7**) [33,34], 8α-(2-methylacryloyloxy)-hirsutinolide-13-*O*-acetate (**8**) [33,34], vernolide-B (**9**) [24], 8α-hydroxyhirsutinolide (**10**) [27], and vernolide-A (**11**) [24], loliolide (**12**) [35], isololiolide (**13**) [35], (3*R*)-3-hydroxy-ionone (**14**) [36], apigenine (**15**) [37], (9*Z*,12*S*,13*S*)-dihydroxy-9-octadecanoic acid (**16**) [38] by comparison of their physical and spectral data with published values. To the best of our knowledge, compounds **12 14** and **16** were isolated for the first time from this plant source.

In the previous phytochemical investigation [27], we reported that all of the sesquiterpene lactones inhibited potently against the TNF-α-induced NF-κB activity and nitric oxide (NO) production in LPS-stimulated RAW 264.7 cells. In the present study, compounds **1 16** were evaluated for their inhibitory effects against aberrant STAT3 activity in the U251MG glioblastoma cancer cell and MDA-MB-231 breast cancer cells, and the viability of the two tumor lines that harbour constitutively-active STAT3, compared to normal NIH-3 T3 mouse fibroblast. As compared with the blank, control compounds **4** and **7 9** showed 64% to 88% inhibitory effects against the viability of U251MG glioblastoma cell line. Compound **7** showed similar inhibitory effects in all of the tested cell lines. Compounds **2** and **6** showed weak inhibitory effect in the U251MG glioblastoma cell line. However, the other compounds were inactive in the tested cell lines (Table 3). Further, treatment of U251MG or MDA-MB-231 cells with compound **7** inhibited intracellular phospho-Tyrosine STAT3 (pY705STAT3) (Fig. 4), suggesting the potential that inhibition of aberrant STAT3 activity in the tumor cells contributes to the loss of viability induced by two compounds.

A variety of sesquiterpene lactones have been known to possess considerable anti-inflammatory activity. Several studies for sesquiterpene lactones have provided an evidence that DNA binding of NF-κB was prevented by alkylation of cysteine-38 in the p65/NF-κB subunit [39,40]. There are strong indications that this is a general mechanism for sesquiterpene lactones, which possess α,β-unsaturated carbonyl structures such as α-methylene-γ-lactones or α,β-unsaturated cyclopentenones. These functional groups are known to react with nucleophiles, especially with the sulfhydryl group of cysteine, in a Michael-type addition [41]. In a recent study, two sesquiterpene lactones, dehydrocostuslactone and costunolide were reported to induce a rapid drop in intracellular glutathione content and consequently inhibited the tyrosine-phosphorylation of STAT3 in cells treated with IL-6, while, dihydrocostunolide, a structural analogue of costunolide lacking only the α,β-unsaturated carbonyl group failed to exert inhibitory action toward STAT3 tyrosine phosphorylation, indicating that this unsaturation in the lactone ring may play a pivotal role in its biochemical activity [42]. Studies of germacranolide type sesquiterpene lactones, costunolide and parthenolide, herein show that these are generally toxic to U251MG and normal NIH3T3 irrespective of the pSTAT3 status. Further, the

inhibition of pSTAT3 at 5 μM was negligible or weak, compared to compound **7**. These results suggest costunolide and parthenolide likely have broad effects on multiple targets.

Hirsutinolide-type sesquiterpene lactones, **1**–**11** isolated from *V. cinerea* possess an *α,β*-unsaturated-*γ*-lactone ring and a 1*β*,4*β*-expoxy group as common functional groups. Although the structure–activity relationship of the sesquiterpene lactones has not been investigated thoroughly, our results suggest the hirsutinolide type sesquiterpene lactone possessing an *α,β*-unsaturated-*γ*-lactone moiety and an ester carbonyl group at C-13 position may enhance the STAT3 inhibitory activity in these cancer cell lines.

Supplementary Material

Refer to Web version on PubMed Central for supplementary material.

Acknowledgments

This study was supported by the National Cancer Institute Grant CA161931 (J.T) and the University of Hawaii, Manoa (J.T). This work was also supported by the NCRR INBRE Program P20 RR016467 (L.C.C), Hawaii Community Foundation (L.C.C) and the National Research Foundation of Korea Grant funded by the Korean Government (Ministry of Education, Science and Technology) (NRF-2011-357-E00071) (to U.J.Y). We are grateful to Drs. R. Borris and A. Wright, Department of Pharmaceutical Sciences, College of Pharmacy, UHH, for providing the NMR spectroscopic and Mass Spectrometry Facility used in this study.

References

1. Bishop JM. Molecular themes in oncogenesis. Cell. 1991; 64:235–8. [PubMed: 1988146]
2. Bromberg JF, Wrzeszczynska MH, Devgan G, Zhao Y, Pestell RG, Albanese C, et al. Stat3 as an oncogene. Cell. 1999; 98:295–303. [PubMed: 10458605]
3. Karin M. Nuclear factor-κB in cancer development and progression. Nature. 2006; 441:431–6. [PubMed: 16724054]
4. Karin M. NF-κB and cancer: mechanisms and targets. Mol Carcinog. 2006; 45:355–61. [PubMed: 16673382]
5. Yu H, Kortylewski M, Pardoll D. Crosstalk between cancer and immune cells: role of STAT3 in the tumour microenvironment. Nat Rev Immunol. 2007; 7:41–51. [PubMed: 17186030]
6. Karin M, Cao Y, Greten FR, Li ZW. NF-κB in cancer: from innocent bystander to major culprit. Nat Rev Cancer. 2002; 2:301–10. [PubMed: 12001991]
7. Karin M, Lin A. NF-κB at the crossroads of life and death. Nat Immunol. 2002; 3:221–7. [PubMed: 11875461]
8. Haura EB, Turkson J, Jove R. Mechanisms of disease: Insights into the emerging role of signal transducers and activators of transcription in cancer. Nat Clin Pract Oncol. 2005; 2:315–24. [PubMed: 16264989]
9. Karin M, Lawrence T, Nizet V. Innate immunity gone awry: linking microbial infections to chronic inflammation and cancer. Cell. 2006; 124:823–35. [PubMed: 16497591]
10. Darnell JE, Kerr IM, Stark GR. Jak-STAT pathways and transcriptional activation in response to IFNs and other extracellular signaling proteins. Science. 1994; 264:1415–21. [PubMed: 8197455]
11. Karin M, Greten FR. NF-κB: linking inflammation and immunity to cancer development and progression. Nat Rev Immunol. 2005; 5:749–59. [PubMed: 16175180]
12. Balkwill F, Mantovani A. Inflammation and cancer: back to Virchow? Lancet. 2001; 357:539–45. [PubMed: 11229684]
13. Coussens LM, Werb Z. Inflammation and cancer. Nature. 2002; 420:860–7. [PubMed: 12490959]
14. Dictionnaire des plantes utiliesees au. Cambodge: Olympic, Phnom Penh; 2000. p. 915
15. Flora of British India III. London: L. Reeve and Co. Ltd; 1882. p. 233

16. Kirtikar, KR.; Basu, BD. Indian Medicinal Plants, II. India: New Connaught Place, Dehradun; 1975. p. 1322
17. Jain SP, Puri HS. Ethnomedicinal plants of Jaunsar-Bawar hills, Uttar Pradesh, India. J Ethnopharmacol. 1984; 12:213–22. [PubMed: 6521494]
18. Chea A, Hout S, Long C, Marcourt L, Faure R, Azas N, et al. Antimalarial activity of sesquiterpene lactones from *Vernonia cinerea*. Chem Pharm Bull. 2006; 54:1437–9. [PubMed: 17015985]
19. Tandon M, Shukla YN, Tripathi AK, Singh SC. Insect antifeedant principles from *Vernonia cinerea*. Phytother Res. 1998; 12:195–9.
20. Pratheeshkumar P, Kuttan G. Effect of vernolide-A, a sesquiterpene lactone from Vernonia cinerea L. on cell-mediated immune response in B16F-10 metastatic melanoma-bearing mice. Immunopharmacol Immunotoxicol. 2011; 33:533–8. [PubMed: 21247369]
21. Grainger CR. Medicinal plants of Seychelles. J Roy Soc Health. 1996; 116:107–9. [PubMed: 8627585]
22. Dastur, JF. Medicinal plants of India and Pakistan. India: D.B. Taraporevala Sons and Co. Private Ltd; 1977. p. 174
23. Dhar ML, Dhar MM, Dhawan BN, Mehrotra BN, Ray C. Screening of Indian plants for biological activity: I. Indian J Exp Biol. 1968; 6:232–47. [PubMed: 5720682]
24. Kuo YH, Kuo YJ, Yu AS, Wu MD, Ong CW, Kuo LMY, et al. Two novel sesquiterpene lactones, cytotoxic vernolide-A and -B, from *Vernonia cinerea*. Chem Pharm Bull. 2003; 51:425–6. [PubMed: 12672998]
25. Gunasingh C, Barnabas G, Nagarajan S. Flavonoids of the flowers of *Vernonia cinerea*. Indian J Pharm Sci. 1981; 43:114.
26. Misra TN, Singh RS, Upadhyay J, Srivastava R. Isolation of a natural sterol and an aliphatic acid from *Vernonia cinerea*. Phytochemistry. 1984; 23:415–7.
27. Youn UJ, Park EJ, Kondratyuk TP, Simmons CJ, Borris RP, Tanamatayarat P, et al. Anti-inflammatory sesquiterpene lactones from the flower of *Vernonia cinerea*. Bioorg Med Chem Lett. 2012; 22:5559–62. [PubMed: 22850207]
28. Zhang X, Yue P, Fletcher S, Zhao W, Gunning PT, Turkson J. A novel small-molecule disrupts Stat3 SH2 domain-phosphotyrosine interactions and Stat3-dependent tumor processes. Biochem Pharmacol. 2010; 79:1398–409. [PubMed: 20067773]
29. Zhao W, Jaganathan S, Turkson J. A cell-permeable Stat3 SH2 domain mimetic inhibits Stat3 activation and induces antitumor cell effects in vitro. J Biol Chem. 2010; 285:35855–65. [PubMed: 20807764]
30. Turkson J, Bowman T, Garcia R, Caldenhoven E, De Groot RP, Jove R. Stat3 activation by Src induces specific gene regulation and is required for cell transformation. Mol Cell Biol. 1998; 18:2545–52. [PubMed: 9566874]
31. Turkson J, Zhang S, Palmer J, Kay H, Stanko J, Mora LB, et al. Inhibition of constitutive signal transducer and activator of transcription 3 activation by novel platinum complexes with potent antitumor activity. Mol Cancer Ther. 2004; 3:1533–42. [PubMed: 15634646]
32. Turkson J, Kim JS, Zhang S, Yuan J, Huang M, Glenn M, et al. Novel peptidomimetic inhibitors of signal transducer and activator of transcription 3 dimerization and biological activity. Mol Cancer Ther. 2004; 3:261–9. [PubMed: 15026546]
33. Borkosky S, Bardon A, Catalan Cesar AN, Diaz JG, Herz W. Glaucolides, hirsutinolides and other sesquiterpene lactones from *Vernonanthura pinguis*. Phytochemistry. 1997; 44:465–70.
34. Jakupovic J, Banerjee S, Castro V, Bohlmann F, Schuster A, Msonthi JD, et al. Poskeanolide, a seco-germacranolide and other sesquiterpene lactones from Vernonia species. Phytochemistry. 1986; 25:1359–64.
35. Park KE, Kim YA, Jung HA, Lee HJ, Ahn JW, Lee BJ, et al. Three norisoprenoids from the brown alga *Sargassum thunbergii*. J Korean Chem Soc. 2004; 48:394–8.
36. Perez C, Trujillo J, Almonacid LN, Trujillo J, Navarro E, Alonso SJ. Absolute structures of two new C13-norisoprenoids from *Apollonias barbujana*. J Nat Prod. 1996; 59:69–72.

37. Wada H, Satake T, Murakami T, Kojima T, Saiki Y, Chen CM. Chemical and chemotaxonomic study of pteridophytes. LIXStudies of the chemical constituents of *Alsophila spinulosa*. Tryon Chem Pharm Bull. 1985; 33:4182–7.

38. Gardner HW, Hou CT, Weisleder D, Brown W. Biotransformation of linoleic acid by Clavibacter sp. ALA2: heterocyclic and heterobicyclic fatty acids. Lipids. 2000; 35:1055–60. [PubMed: 11104009]

39. Garcia-Pineres AJ, Castro V, Mora G, Schmidt TJ, Strunck E, Pahl HL, et al. Cysteine 38 in p65/NF-κB plays a crucial role in DNA binding inhibition by sesquiterpene lactones. J Biol Chem. 2001; 276:39713–20. [PubMed: 11500489]

40. Garcia-Pineres AJ, Lindenmeyer MT, Merfort I. Role of cysteine residues of p65/NF-κB on the inhibition by the sesquiterpene lactone parthenolide and *N*-ethyl maleimide, and on its transactivating potential. Life Sci. 2004; 75:841–56. [PubMed: 15183076]

41. Schmidt TJ. Toxic activities of sesquiterpene lactones: structural and biochemical aspects. Curr Org Chem. 1999; 3:577–608.

42. Butturini E, Cavalieri E, Carcereri de Prati A, Darra E, Rigo A, Shoji K, et al. Two naturally occurring terpenes, dehydrocostuslactone and costunolide, decrease intracellular GSH content and inhibit STAT3 activation. PLoS One. 2011; 6:e20174. [PubMed: 21625597]

Appendix A. Supplementary data

Supplementary data to this article can be found online at http://dx.doi.org/10.1016/j.fitote.2013.12.013.

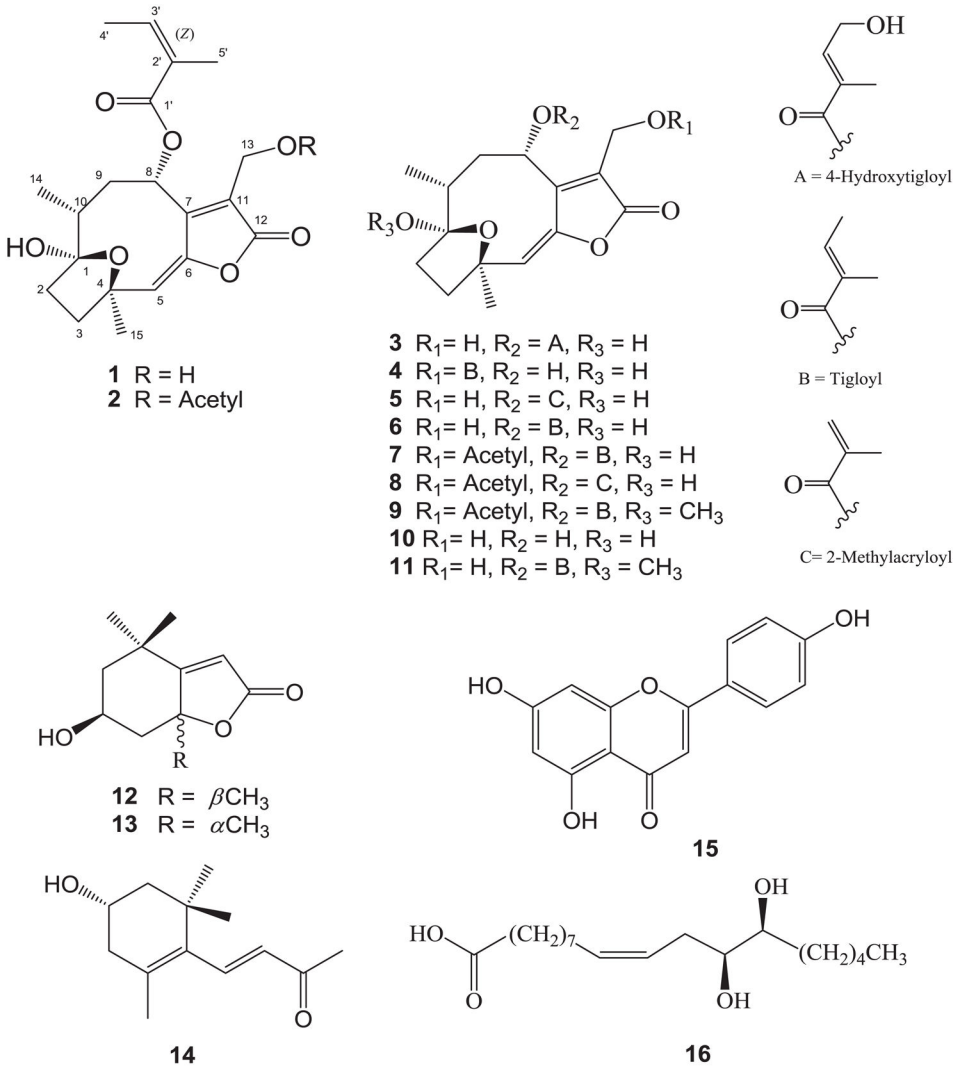

Fig. 1.
Structures of compounds **1**–**16**.

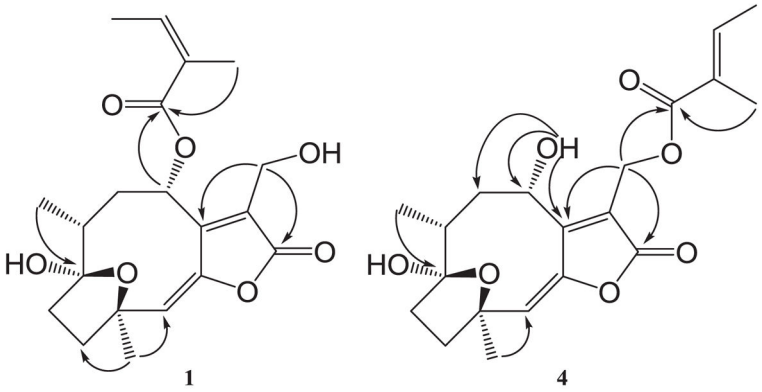

Fig. 2.
Important HMBC correlations of compounds **1** and **4**.

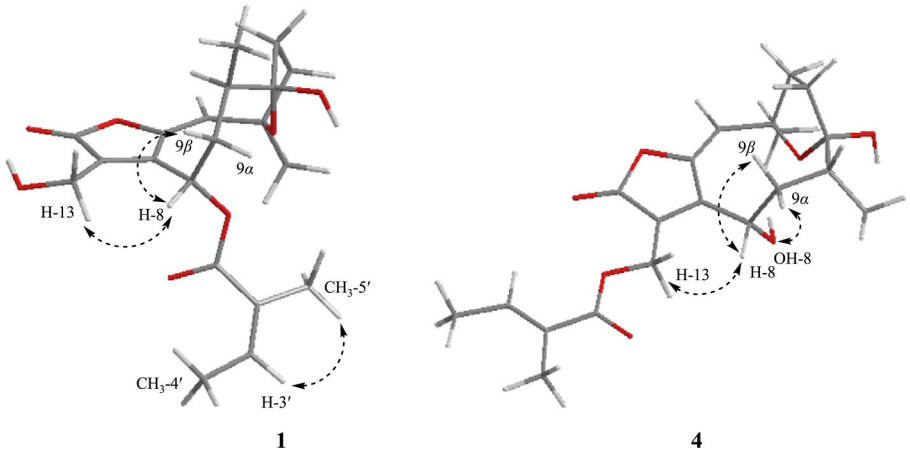

Fig. 3.
Key NOESY correlations of compounds **1** and **4**.

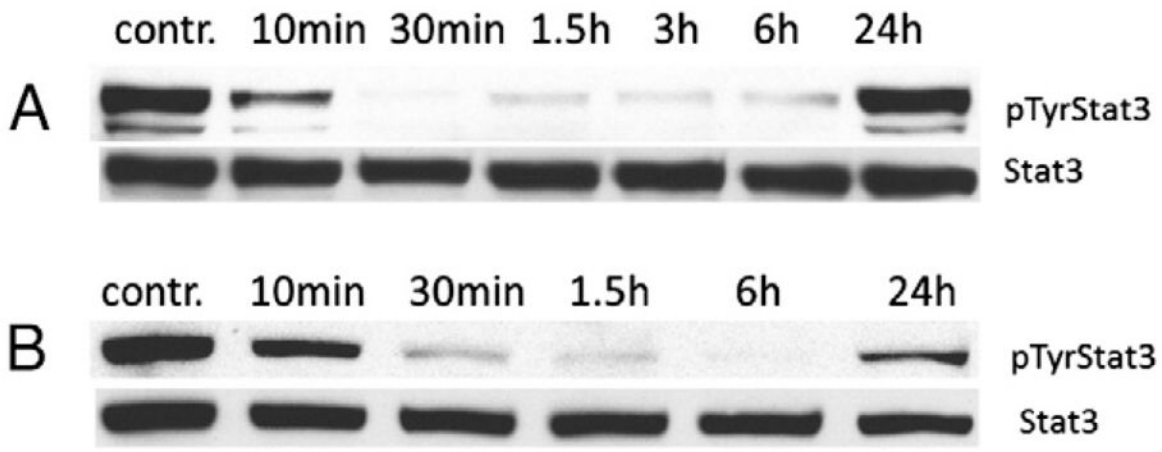

Fig. 4.

Compound **7** (5 μM) inhibited STAT3 phosphorylation in U251MG (A) and MDA-MB-231 (B) cells, as detected by Western blot analysis-acetate inhibits STAT3 activation.

Table 1

NMR data (400 MHz, in $CDCl_3$) for compounds **1** and **2.**

Position	1		2	
	$\delta_{H,\ mult.\ (J\ in\ Hz)}$	δ_C	$\delta_{H,\ mult.\ (J\ in\ Hz)}$	δ_C
1		108.0		107.8
2	2.16, m[a]	38.5	2.10, m[a]	38.1
3	2.16, m[a]	38.6	2.10, m[a]	39.2
4		81.2		83.4
5	5.87, s	125.6	5.90, s	126.1
6		146.4		145.5
7		147.5		150.8
8	6.34, d (8.0)	68.2	6.28, d (10.8)	68.3
9α	2.36, dd (15.6, 11.6)	37.9	2.36, dd (15.6, 12.0)	35.4
9β	1.87, m		1.83, m	
10	1.90, m	41.3	1.88, m	41.3
11		131.6		128.8
12		169.4		167.8
13a	4.65, d (13.2)	54.4	5.12, d (12.4)	55.5
13b	4.56, d (13.2)		5.05, d (12.4)	
14	0.97, d (6.8)	16.8	0.97, d (7.6)	16.6
15	1.48, s	27.9	1.50, s	29.4
1′		170.4		170.8
2′		128.2		126.9
3′	6.17, q (7.6)	139.9	6.10, q (8.8)	138.1
4′	2.02, d (7.6)	15.9	2.01, d (8.4)	15.8
5′	1.93, s	20.6	1.92, s	19.0
$\underline{C}OCH_3$				170.7
$CO\underline{CH_3}$			2.10, s	20.9

Chemical shift (δ) are in ppm, and coupling constants (J in Hz) are given in parentheses.

[a]Overlapping signals.

Table 2

NMR data (400 MHz, in CD_3OD) for compounds **3** and **4.**

Position	3[a]		4[b]	
	$\delta_{H,\ mult.\ (J\ in\ Hz)}$	δ_C	$\delta_{H,\ mult.\ (J\ in\ Hz)}$	δ_C
1		107.9		109.1
2*α*	2.06, m[c]	37.3	2.20	37.0
2*β*			2.07	
3	2.12, m[c]	38.0	2.24, m[c]	38.4
4		80.6		80.9
5	5.99, s	126.4	5.86, s	123.7
6		146.2		146.2
7		149.1		154.9
8	6.43, d (8.0)	69.1	5.19, dd (11.6, 6.0)	66.5
9*α*	2.40, dd (14.0, 12.0)	35.4	2.24, m[c]	38.1
9*β*	1.94		1.84, m	
10	1.91, m	41.6	1.94, m	40.4
11		133.5		133.7
12		168.2		166.8
13	4.50, s	52.9	4.97, s	55.0
14	0.93, d (6.8)	16.0	0.95, d (7.6)	17.3
15	1.51, s	27.0	1.61, s	28.4
1′		167.6		167.1
2′		127.3		127.4
3′	7.08, t (6.4)	142.3	6.88, q (6.8)	138.6
4′	4.28, d (6.4)	58.4	1.81, d (6.8)	14.4
5′	1.84, s	11.2	1.84, s	12.0
OH-8			6.15, d (11.6)	

[a] Spectra recorded at ^1H (400 MHz) and ^{13}C NMR (100 MHz) in CD_3OD.

[b] Spectra recorded at ^1H (400 MHz) and ^{13}C NMR (100 MHz) in $CDCl_3$.

[c] Overlapping signals.

Table 3

STAT3 inhibition effect of compounds **1 16.**

	U251MG[a]	MDA-MB-231[b]	NIH-3T3[c]
Compounds	**% inhibition[d]**	**% inhibition**	**% inhibition**
Control	ne[e]	ne	ne
1	ne	ne	ne
2	48.6	ne	8.0
3	ne	ne	ne
4	80.9	26.2	32.1
5	ne	ne	ne
6	18.0	15.0	ne
7	88.8	81.7	76.0
8	64.8	37.8	50.7
9	67.7	14.0	ne
10	6.0	ne	ne
11	ne	ne	ne
12	ne	ne	ne
13	nd[f]	nd	nd
14	ne	ne	ne
15	ne	ne	ne
16	ne	ne	ne
costunolide	17.5	10.5	41.6
parthenolide	52.0	18.7	79.4

Control measurement was performed with the solubilising agent (DMSO),

[a] glioblastoma cancer cell,

[b] breast cancer cell,

[c] mouse fibroblast cell,

[d] % inhibition at 5 μM,

[e] ne, no effect inhibition,

[f] nd, not determined.